AFM investigation of Martian soil simulants on micromachined Si substrates

S. VIJENDRAN, H. SYKULSKA & W. T. PIKE
Optical and Semiconductor Devices Group, Electrical and Electronic Engineering, Imperial College London, Exhibition Road, London SW7 2BT, UK

Summary

The micro and nanostructures of Martian soil simulants with particles in the micrometre-size range have been studied using a combination of optical and atomic force microscopy (AFM) in preparation for the 2007 NASA Phoenix Mars Lander mission. The operation of an atomic force microscope on samples of micrometre-sized soil particles is a poorly investigated area where the unwanted interaction between the scanning tip and loose particles results in poor image quality and tip contamination by the sample. In order to mitigate these effects, etched silicon substrates with a variety of features have been used to facilitate the sorting and gripping of particles. From these experiments, a number of patterns were identified that were particularly good at isolating and immobilizing particles for AFM imaging. This data was used to guide the design of micromachined substrates for the Phoenix AFM. Both individual particles as well as aggregates were successfully imaged, and information on sizes, shapes and surface morphologies were obtained. This study highlights both the strengths and weaknesses of AFM for the potential *in situ* investigation of Martian soil and dust. Also presented are more general findings of the limiting operational constraints that exist when attempting the AFM of high aspect ratio particles with current technology. The performance of the final designs of the substrates incorporated on Phoenix will be described in a later paper.

1. Introduction

Atomic force microscopy (AFM) has become a versatile tool for the study and manipulation of structures at the nanoscale. Applications range from surface characterization in material science, to the study of living biological systems in their natural environment, to nanolithography. AFMs are even finding uses in the field of space exploration,

specifically for the in situ investigations of dust and soil particles from comets/asteroids or on the surface of planetary bodies. The European Rosetta spacecraft, on the way to Comet 67P/Churyumov-Gerasimenko, carries an AFM as part of its Micro-Imaging Dust Analysis System. It aims to conduct microtextural and statistical analysis of cometary dust particles (Riedler *et al.*, 1998). The Phoenix spacecraft, which will land on Mars as part of NASA's Phoenix mission launching in 2007 will also carry an AFM, which will be part of a microscopy station that includes an optical microscope. This AFM, dubbed the 'First AFM on MARS' or FAMARS, will contribute to the aims of the Phoenix mission by measuring the sizes, shapes and surface textures of soil and dust particles for clues on the history of water at the Northern latitudes of Mars. Experiments from previous Mars lander missions have indicated that the average size of the airborne particles at the Martian surface is between 1 and 3 μm (Landis *et al.*, 1996). At this small scale, *in situ* optical microscopy, such as that being performed by the Microscopic Imagers (30 μm per pixel) on the two Mars Exploration Rovers is insufficient to resolve the individual particles. As such, *in situ* scanning electron microscopes (SEM) or AFMs are the better options for interrogating samples at these length scales. However, miniaturization of an SEM for planetary exploration has thus far been an elusive goal due to the complexity of such a system. Furthermore, the insulating properties of the particles under study would present additional difficulties to electron microscopy. By contrast, the AFM is able to operate in the ambient environment on Mars, on non-conducting samples, and can provide 3D information of a sample. In order to obtain clues about particle transport history, the dimensions, shapes and surface features of the grains need to be determined. FAMARS will be able to provide data on these important parameters including particle diameters (up to 40 μm), heights (up to 6 μm) and surface roughness/texture (lateral resolution of 10 nm/pixel for a 5 μm scan area), thereby addressing length scales unattainable with any other previous or current *in situ* planetary exploration instrument. Crucially,

the AFM images will show surface texture and patterning at a level of detail not hitherto possible on Mars, which, together with other contextual data from the optical microscope and chemistry instruments, will help in determining the weathering mechanisms and transport history of the particles and could further strengthen the case for past or present water on Mars (Kempe *et al.*, 2004). Aeolian and aquatic transport for example, can be differentiated by AFM observation of the microstructure of the particles as the former produces pitting of the surface whereas the latter results in chemical dissolution of minerals along crystal planes. The AFM will also be able to measure the sizes of the dust grains suspended in the Martian atmosphere which have a big impact on the solar radiation balance of Mars and hence are of critical importance in climatological models (Gierasch and Goody, 1968; Kahn *et al.*, 1992). Additionally, dust is likely to be one of the major hazards for future human explorers, as it can contaminate suits and equipment, lead to electrical discharges and interfere with radio communications. (Horneck *et al.*, 2001).

1.1. AFM imaging of micrometre-sized particles

The important difference between the operating conditions that are likely to be experienced by the Rosetta and Phoenix AFMs, is that for the Rosetta mission, the cometary particles are expected to be in the *submicrometre* size range (Riedler *et al.*, 1998). By contrast, on Mars, the mean size of the wind-borne dust grains is estimated to be 1–3 µm (Landis *et al.*, 1996), whereas the soil particles on and below the surface have a distribution of sizes from submicrometres to millimetres or more (Soderblom *et al.*, 2004). In order to be able to study particles at high spatial resolution, the instrumentation constrains the maximum size of particle that can be imaged: the optical microscope with a resolution of 4 µm has a depth of field of 80 µm, whereas the AFM has a maximum height range of 14 µm. Hence, the size distribution of the particles delivered to the microscopes by the robotic arm on Phoenix will be limited by scraping off most of the material from the substrates, leaving a layer that is only 200 µm thick. Thus, the maximum particle height that can be imaged on a flat substrate by the optical and atomic force microscopes will be of the order of 200 µm with both microscopes only able to image a portion of such a particle in a single acquisition.

Despite this sample preparation, there still remains the question of how well the AFM on Mars will cope in imaging samples with this range of particles sizes. One of the limitations of scanning probe microscopy techniques is that the probes interact by contact with the sample and due to the mechanical limits of the size of the probes, this limits the sizes or roughnesses of the particles they can measure. For smooth surfaces (mean roughness <100 nm), only the end of the probe interacts with the surface features, and hence only the probe radius is important. However, for rough surfaces, multiple points on the probe may be simultaneously in contact

with the surface features and so the geometry of the tip has a large affect on the accuracy of the imaging. Tip artefact in the image can greatly distort and mask actual features and make the interpretation of the data difficult. Typical silicon AFM probes have tips that are about 10 µm in height, and are tetrahedrally shaped, when fabricated with the most common techniques. Although the end of the apex of the tip may have a radius of only 10 nm or less, the overall tetrahedral shape limits the aspect ratios to very low values. As such, these tips are excellent for studying topography in the nanometre height range, but are extremely limited when faced with features in the micrometre range. In fact, there is very little evidence in the literature of work that has been done with AFMs on 1 to 10 µm-high features, except in the area of metrology of semiconductor device processing (photoresist and trench profiling) (Ridley *et al.*, 2002). For these applications, special tips with high aspect ratios are required, including exotic tips such as carbon nanotubes (Bhushan *et al.*, 2004). Alternatively, a 'hopping' approach to the *X-Y* scanning of the AFM has been shown to help reduce tip-sample convolution (Hosaka *et al.*, 2002). The Phoenix AFM (Akiyama *et al.*, 2001; Pike *et al.*, 2001) however, being a space-qualified instrument, is limited in its range of available tip geometries, as robustness is a key criteria for space-bound hardware, and high-aspect ratio tips tend to be very fragile and more difficult to use.

In relation to the study of particle morphology, some work has been done on the determination of surface texture/roughness with the AFM (Barkay *et al.*, 2005) and also in the search for extraterrestrial fossils in Martian rock (Steele *et al.*, 1998). However, these studies have tended to focus only on very small and relatively smooth (<1 µm roughness) areas of much larger samples. There have been precious little, if any, studies on AFM imaging of individual micrometre-sized particles in their entirety, outside of the work done by Gautsch *et al.* (2002) during initial qualification of FAMARS for the cancelled 2001 Mars Surveyor Lander mission. This work was probably the first to highlight the difficulties in AFM scanning of micrometre-sized loose particles, although they were able to image a number of <5 µm quartz particles to demonstrate the capabilities of the FAMARS instrument.

Another limitation of AFM when it is used to image loose, micrometre-sized particles is the minimum lateral force that is applied to the sample during scanning. Although the lateral force between the end of the tip and a relatively flat (<100 nm roughness) sample surface can be greatly reduced when operating in the dynamic mode, this does not remove the possibility of the side of the tip contacting tall (>1 µm) features if scan speeds are too high. This is due to the fact that the response time of the feedback loop that controls the cantilever's z-position is limited by the speed of the z-actuator and the *Q*-factor of the cantilever. For a typical oscillating cantilever with a resonant frequency in the 100's of kHz range and a *Q* of a few hundred, close-loop feedback times can be
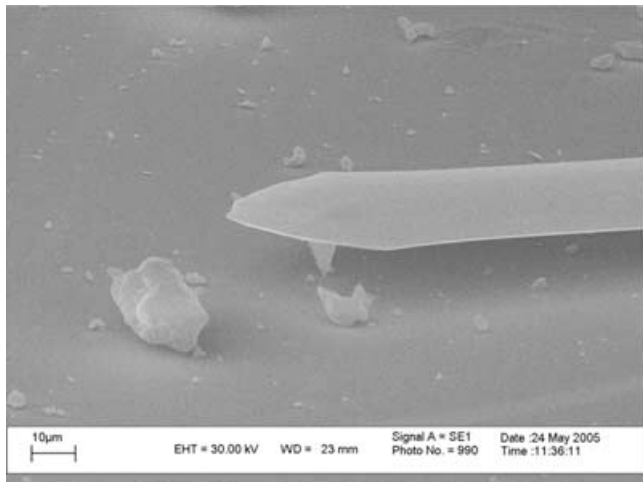
Fig. 1. Caption: SEM micrograph of one of our AFM cantilevers on a Si substrate surrounded by particles in the typical size range (> 1 m) that we are attempting to image. The difficulty of safely scanning large areas of the substrate when such large particles are present is clear from this image. The scale bar is 10 μm.

Fig. 2. Caption: AFM image of Mars-1 particles embedded in photoresist. The image was obtained in dynamic mode with a scan speed of more than 6 m s^{-1}. The particles are sufficiently immobilized for high resolution imaging.

greater than a millisecond. Consequently, when imaging loose particles at speeds greater than about 5 m s^{-1}, the dynamic mode with z-feedback control has little effect in reducing the lateral force on the particles when the tip encounters steep upward slopes. Figure 1 is a SEM image of an AFM cantilever and tip surrounded by a number of particles, some of which are as large as the AFM tip itself. We have repeatedly found in our experiments, that whenever flat, hard substrates are used, we are unable to image micron-sized particles with much success, especially when scan speeds are > 5 m s^{-1}. These difficulties with particle movement by the tip were similarly observed by Gautsch *et al.*, during their work with quartz particles on a polymer substrate (Gautsch *et al.*, 2002).

In the laboratory setting, the obvious solutions to these problems are to slow down the scan speed or to use substrates with adhesive coatings to hold down the particles (Resch *et al.*, 2001). With regard to slow scan speeds, during a space mission, there is a minimum practicable speed that depends on the detail required in the image and the finite time that is available for the experiments. In the case of Phoenix for example, the time budgeted for the AFM is such that with scan times of about 30 min per image (scan speeds of less than 10 m s^{-1}, scan range of 40 μm, 256 × 256 lines), the total number of images returned during the mission will be about a few hundred at most. Although this sounds like a small number compared to typical data returned from other imaging instruments such as the Microscopic Imager on the Mars Exploration Rovers, much can be learned from just a few 3D images of particle structure at the microscale, as we demonstrate later. However, if the scan speed or resolution is reduced further, this would limit the scientific utility of the AFM instrument during this mission. Therefore, it is imperative that we obtain
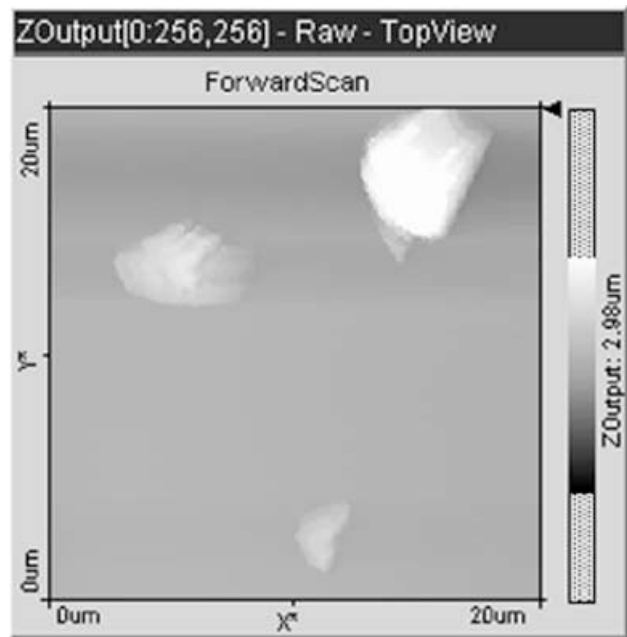
suitable scanning conditions that allow a reasonable scan speed without disturbing the target particles.

In terms of increasing the adhesion to the surface, this can be done in the laboratory by careful choice of adhesive coatings on the substrates. Figure 2 shows a flat Si substrate coated with 1 μm of unbaked photoresist on which particles of JSC Mars-1 were deposited. Particles were successfully imaged with scan speeds of up to 6.5 m s^{-1} without any evidence of particle movement.

However, for the Phoenix mission, the very cold (∼ −40 °C) and dry environment on the Martian surface precludes the use of such adhesive coatings, as most known adhesives have higher glass transition temperatures than −40 °C. Even the normally present thin film of water that is prevalent in ambient terrestrial AFM experiments is not available to assist with adhesion at these low temperatures and humidities. Therefore, the remaining mechanisms for particle adhesion to a substrate are:

1. Short-range Van der Waals forces,
2. Electrostatic attraction from triboelectric or contact charging,
3. Atomic interdiffusion through contact,
4. Magnetic forces and
5. The mechanical gripping of particles by high-aspect-ratio topography.

Some of these mechanisms, including short-range Van der Waals and magnetic forces are utilized by other substrate types (silicone, strong and weak magnets) included in the

Phoenix microscopy station. In this paper, our investigations into some of the other mechanisms are discussed, and the utility of patterned silicon substrates (some of which have also been included on Phoenix) is demonstrated in the context of combining optical microscopy and AFM for imaging micron-sized particles.

2. Experimental method and materials

The Phoenix microscopy station (side view shown in Fig. 3) includes an optical microscope, AFM and a two-degree-of-freedom sample stage. The sample stage consists of 10 identical sets of 5 substrates types (microbucket, strong and weak magnets, silicone and patterned silicon) plus a number of calibration substrates. Note that the samples are mounted vertically relative to the microscopy station when in the scanning position. To allow for the possibility of damage or wear to the AFM tips, the AFM scanner head includes a chip which consists of an array of 8 Si cantilevers (shown in the inset of Fig. 3) with identical tips which can be interchanged autonomously on Mars by the sequential breaking off of the cantilevers and supporting beams as an when it is required. The AFM chip is mounted at a 10° angle relative to the substrates,
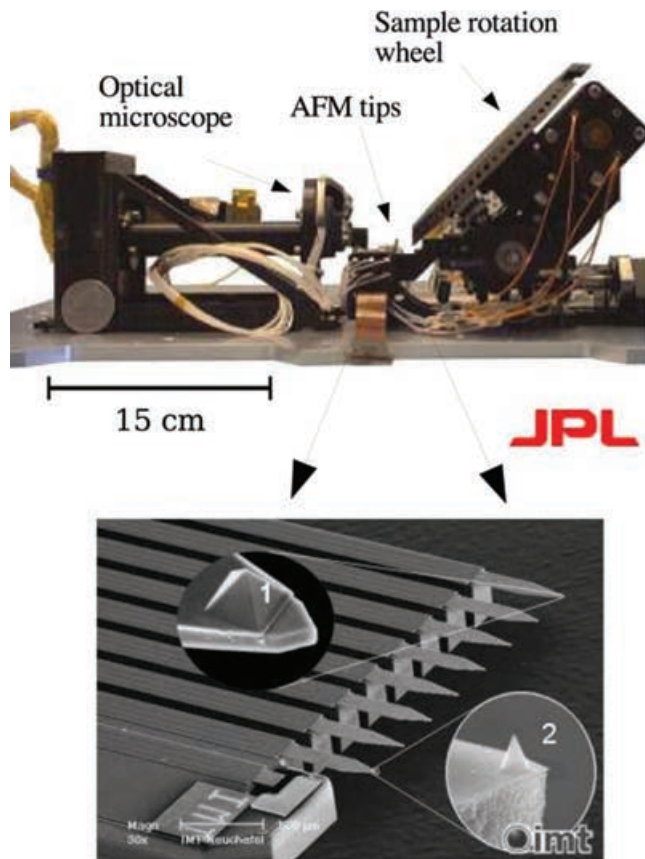
thus only one of the tips of the array is in contact with the sample at a time. For more detailed information on the FAMARS design, refer to (Akiyama *et al.*, 2001).

As a substitute for the flight version of the Phoenix microscopy station, a Nanosurf Easyscan AFM was used for these experiments, as it has a common scanning system and control software with the FAMARS instrument. Cantilevers with Silicon tips from Nanosensors (PPP-NCLR with a radius of 10 nm) were used for all the imaging. The AFM was operated in amplitude modulated dynamic mode, at room temperature and normal humidity, using scan speeds ranging from 10 μm s^{-1} down to 0.7 μm s^{-1}. The amplitude damping setpoint was always set just high enough to allow the tip to track the surface accurately. This AFM does not come with a built in optical microscope, so a separate microscope was used for all the optical microscopy. No evidence of movement of the particles was observed during any of the sample transfers between the AFM and the optical microscope. Sample manipulation was performed with an X-Y linear translation stage with manual micrometres. An image of the apparatus used is shown in Fig. 4.

Several different substrate patterns such as pits and pillars were made using standard silicon processing techniques and
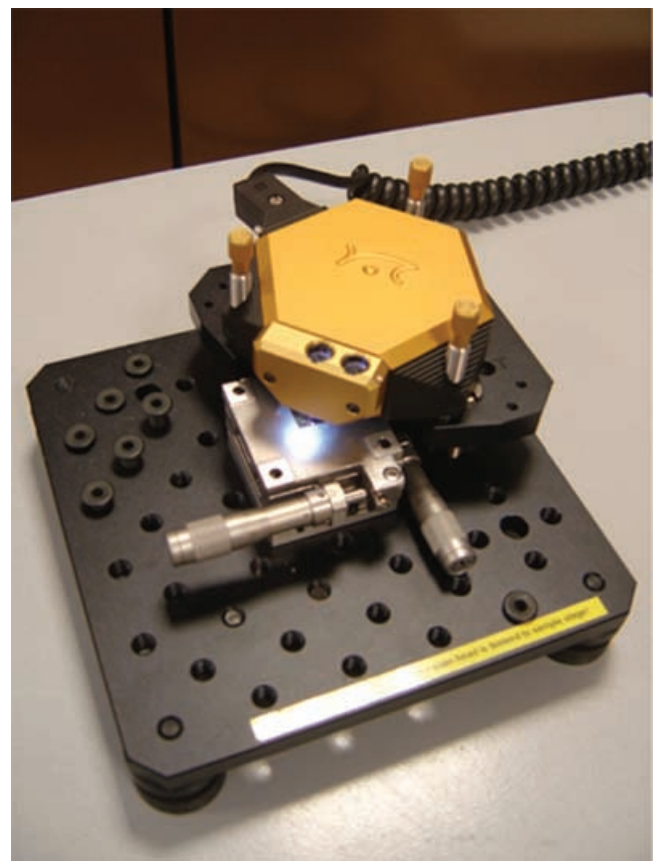

Fig. 3. Caption: The Phoenix microscopy station with the blowup showing the AFM tip array. Images courtesy of the Jet Propulsion Laboratory and the Institute of Microtechnology, Neuchâtel, respectively.

Fig. 4. Caption: Easyscan AFM setup with manual micrometre positioning stage.

reactive ion etching to investigate the effectiveness of different geometries and aspect ratios. We analyzed the substrates with various Martian analogues to examine the effect they had on the adhesion of differently sized and shaped particles. The simulants that were used were:

1. JSC Mars-1 (Allen *et al.*, 1997) (size range from ~1 μm to 1 mm) composed of palagonitic tephra of basaltic composition from Pu'u Nene cinder cone on the Island of Hawaii where the fresh tephra is altered to palagonite via dissolution, oxidation and addition of water, and not by transport;
2. Diatomaceous Earth (composed of fossilized remains of diatoms, mainly in the micrometre size range) and
3. Alumina powder (99% of particles smaller than 10 μm).

To simulate the mechanical sample handling used by the Phoenix spacecraft, particles were deposited on the substrates by dropping samples from a spatula from a height of 2–3 cm onto the oven-dried Si substrates. This resulted in a 2- to 3-mm-high pile of material, which was then rotated through 90° to imitate the vertical scanning position of the substrates on the Mars-AFM. Most of the sample dropped off, then the substrates were returned to the horizontal position for subsequent analysis of the remaining particles. It was assumed that any particles that adhered to the substrates after the initial 90° rotation, would have remained in place even if the subsequent AFM analysis was done with the substrates in the vertical position. It must be noted that when on Mars, the lower Martian gravity of 0.38 g, may result in more particles remaining on the substrates after rotation into the vertical position than in our tests, especially in the larger size range. It is not possible to simulate the effect of the reduced Martian gravity on the particle adhesion in this case, even by rotating the substrate by less than 90°, as there is still a contact force between sample and substrate in the direction of Earth's gravitational pull. However, the room temperature and humidity conditions that we used in our experiments may well have countered the effect of the stronger gravity on Earth by increasing the adhesive force between the particles and the substrate due to the adsorbed water layers on the silicon and particle surfaces. Therefore, the results presented here are based only qualitatively on the size distribution and total number of particles. In addition, the scraping off of the sample material to leave a 200 μm layer was not simulated here either, and this may have also influenced the distribution of the remaining particles towards the smaller size range. Larger particles often form larger aggregates which pry themselves off the substrate surface under their own weight when the substrate is rotated by 90°.

To get a general view of the particle distribution on the samples, an optical microscope was used with a magnification and field of view similar to the Phoenix microscope (6× magnification, 2 × 1 mm field of view). Close up SEM images were also obtained of particles and areas of interest that were subsequently studied with the AFM.

The effect of lab humidity on the adhesion properties between the particles and the substrates was investigated, by comparing samples that had been dried with ones that were at normal humidity. To dry the dust and substrates we dehydrated both in a 150 °C oven for 1 h. We placed the dried dust on a flat substrate and rotated through 90° and observed the particles that were retained. As a control, we performed the same procedure with soil and a substrate that had not been dehydrated. The particle distributions of the remaining soil after 90° rotation were compared under an optical microscope.

3. Results and discussion

3.1. Sorting of particles

A potentially good way of filtering the size of particles that remain on the substrate is by using closely space etched pits such as those shown in Fig. 5. The pit diameter limits the sizes of the particles that can be captured within the pits, whereas the close spacing ensures that there is very little area on the surface of the wafer for larger particles to adhere on to. In this way, the sample loading on the substrate can be controlled to some extent, in the case where too much sample on the substrate may be detrimental to safe AFM operations.

After depositing a spatula of soil on the substrate, it was turned 90° into the vertical position. This resulted in almost all particles larger than the pit diameter (10 μm) falling off. A few large particles or clumps did remain but overall, the etched region was free of particles greater than 10 μm in diameter. The difference in particle density on the etched and flat regions of the substrate however, was only significant for the Alumina (Al_2O_3) sample This was due to the fact that the JSC Mars-1
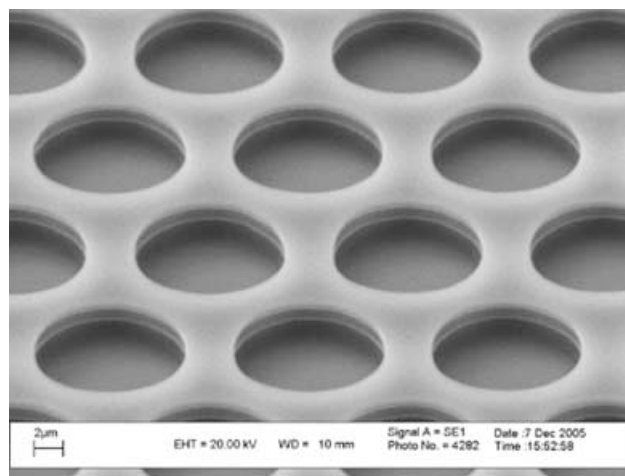

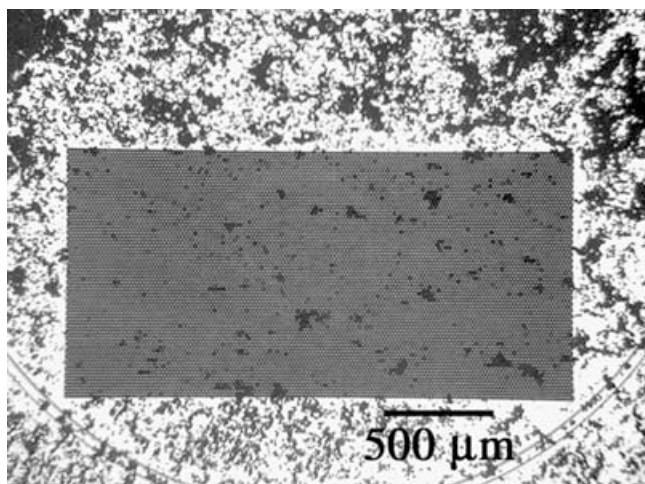**Fig. 5.** Caption: SEM of 10-m-diameter circular pits, with a 14 m pitch, etched 1.5 m deep in Si.

Fig. 6. Caption: Optical image of Al_2O_3 particles on an array of 10-m-diameter pits showing how the adhesion of particles over the etched region is much reduced as compared to that over the flat areas of the substrate. Closely spaced etched pits can thus be used to provide a sparsely populated region of particles for safe AFM scanning. This experiment was conducted with the substrate and sample at normal lab humidity.

particles did not adhere greatly to flat silicon anyway (<3000 particles cm^{-2}), whereas the Diatomaceous Earth particles were sufficiently irregular to maintain adhesion even in the etched regions through the large surface area of the particles. Fig. 6 shows the substrate deposited with Al_2O_3 where the difference between the two regions is obvious.

The result was that the sample loading was greatly reduced (coverage only $\sim 5\%$ or 10000 particles cm^{-2}) compared to the unpatterned regions where the particles adhered to densely (coverage $\sim 50\%$). Individual particles in the patterned region could potentially then be safely approached and scanned with the AFM. Note that in order to image particles in a sparse field (<60000 particles cm^{-2}, i.e. interparticle distance of 40 m or greater), accurate registration is required between the optical microscope and the AFM positioning system to allow commanding of the AFM to approach and image in a particular location. This is due to the limited scan range of the Easyscan AFM which is about 40×40 μm only. Although this is considerably larger than most commercial AFMs, it is still very small compare to an optical microscope. Accurate positioning is available in the Phoenix system (which has a scan range of about 50×50 μm and can be positioned to within a few micrometres); however, it was not possible to do this in our setup which only had a low-magnification built-in lens in the AFM body to allow general tip location to within ± 100 μm by visual observation. Hence, in the current setup, the few AFM images of particles that were successfully obtained, were acquired by scanning in a number of different areas around the substrate until particles were found in the image. Clearly, there is an inevitable trade-off between the safety of the

AFM tip (which would be compromised with a dense field of particles) and successfully locating a number of particles to be scanned.

The importance of a debris-free region around the small particles cannot be overstated. When a substrate is populated by a large number of large particles the successful scanning of the AFM cantilever is severely hampered by collision of the cantilever edge with the particles on the surface. This results from the fact that typical AFM tip heights are only about 10 μm, and so the cantilevers would collide with any particle larger than that size on the surface of the substrate. Therefore, to image a particle without the risk of contaminating or breaking a cantilever, the region surrounding the particle would need to be free of particles >10 μm higher than the substrate surface. It is possible that particles with heights a little more than 10 m may be able to be imaged without damaging the cantilevers if slow scan speeds are used, although the images will undoubtedly include some noise where the cantilever edge first comes into contact with the sides of the particles, before the z-feedback responds and moves the scanner away from the surface. However, this does not preclude using an AFM to image small areas of large particles (>50 μm in diameter), as long as the tip is brought into contact with and remains within a region away from the edges of the particles.

3.2. Gripping of particles

Pits and pillars also serve the important function of immobilizing the particles during AFM scanning. Despite the use of dynamic mode AFM with low setpoints, the effect of the lateral forces on the particle stability during scanning is significant for the smaller particle sizes (sub-100 μm). As mentioned before, the low-temperature environment of the Martian surface precludes the use of adhesive coatings on the substrates to fix the particles in place. Therefore, substrates such as silicone, strong and weak magnets and micromachined silicon with high aspect ratio topography were developed (only the last of which at Imperial College London) to enhance the adhesion of particles for the AFM measurements.

For the micromachined substrates, the aspect ratios of the pits and pillars are important to ensure that some parts of the particles are protruding above the surface of the etched features. This then allows AFM scanning of the top section of the particle, while enough of the particle is in the pit or between the pillars and hence is 'gripped' when the substrate is in the vertical position. A 2:1 diameter-to-depth ratio was found to be effective for this application. This means that roughly half of the particle (assuming a sphere) is inside the pit permitting solid gripping of the particle.

For the smaller particles (<10 μm), the pits and pillars are particularly useful in holding them in position during scanning, as they would otherwise be easily pushed laterally by the tip. Figure 7 shows examples of particles trapped within etched pits and between pillars.
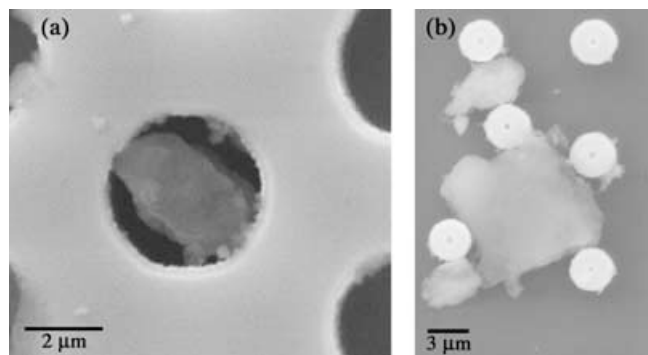
Fig. 7. Caption: SEM micrographs of (a) 5-m-diameter, 5-m-deep etched pits in Si with a particle of JSC Mars-1 simulant immobilized within a pit and (b) JSC Mars-1 particles wedged between 3-m-diameter, 5-m-high pillars.

The pillars are also essential on a silicon substrate for holding onto the largest particles (200 μm) which would otherwise fall off the substrate under their own weight when the substrates are moved into the vertical position (even in the 0.38 g of Martian gravity). Figure 8 shows optical micrographs of a Si substrate, part of which is covered with a reactive ion etching etched grid of circular pillars.

The pillars shown in Fig. 8 were 4 μm in diameter with a pitch of 10 μm and a height of 5 m. From these images, it is clear that there is generally increased adhesion over the patterned region as compared to the surrounding flat substrate especially towards the larger sizes. Therefore, by including both pillars and pits on the same silicon substrate, a sample with a wider range of particle sizes is obtained, providing a better choice of targets for detailed imaging. Also, particles trapped between pillars are in a potentially more stable configuration which should allow improved AFM scanning. This behaviour was observed for all the analogues. As anticipated, the pillars in this configuration behave in exactly the opposite manner to the 10 μm pits shown in Fig. 6, where the etched region holds less large particles compared to the flat areas.

3.3. AFM imaging of small particles

The patterned substrates with closely spaced pits performed very well when we attempted to image particles in the sub-10 μm size range. Figure 9(a) shows a micrograph of a Si substrate with 5 m pits coated with some JSC Mars-1 particles, whereas Fig. 9(b) is an AFM image of a particle in and around one of the pits. The AFM scan was performed from the top of the image downwards, and we can see that there is one particle firmly inside the pit, whereas another is perched partially on the surface and partially in the pit. This latter particle is seen to be moved by the tip approximately half-way through the image, and rescanned in a new position. This nicely demonstrates the effectiveness of pinning down particles in pits to avoid movement by the tip.
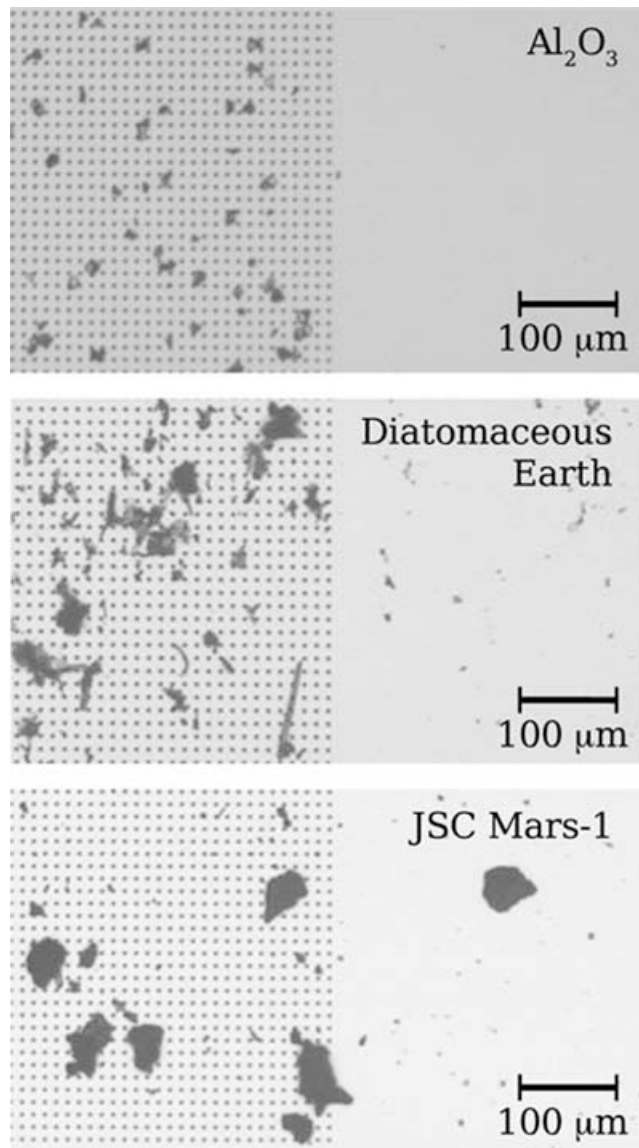

Fig. 8. Caption: Optical micrograph of 4-m-diameter etched Si pillars with 10 m pitch and 5 m height showing increased adhesion of particles in the patterned regions due to the gripping action of the pillar structures. This experiment was conducted with the substrate and sample at normal lab humidity.

3.4. AFM imaging of large particles

The maximum height range of the AFM we used for this work was 12 μm. Therefore, large particles with surface features greater than this height could not be imaged in their entirety. This is a limitation common to all AFMs, more so those capable of higher resolutions than with the Easyscan AFM. As such, the utility of an AFM in imaging particles of this size is in the measurement of surface texture over small areas of the particles, which can give information of weathering processes (aeolian or water) and transport history (Kempe *et al.*, 2004).
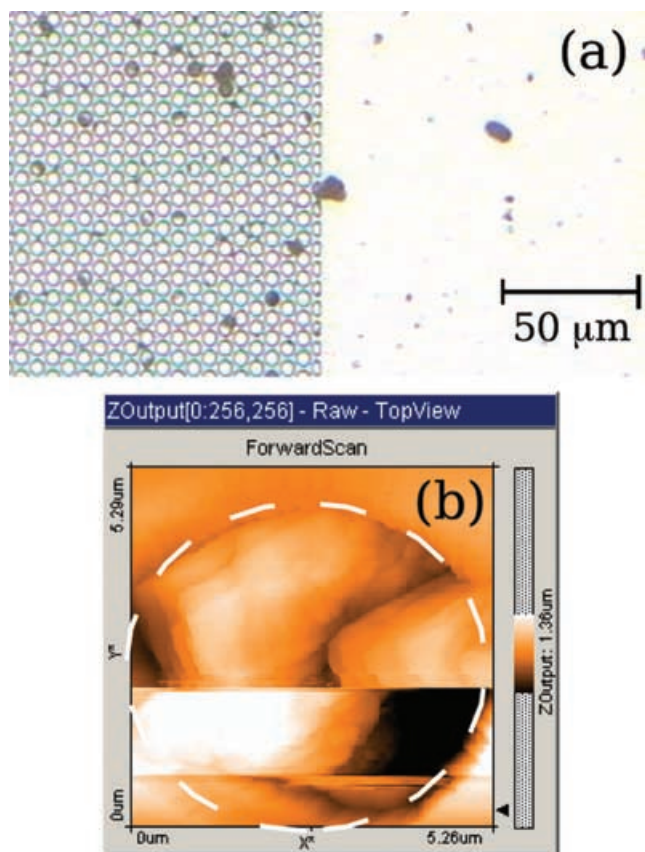
Fig. 9. Caption: (a) is an optical micrograph of 5 m pits with a coating of JSC Mars-1 particles. (b) is an AFM image of particles in and around one of the pits. The image was scanned from top to bottom. The white dashed line is a guide to the eye showing the edge of the pit. The particle outside the pit (on the right-hand side of image) is easily moved by the scanning tip despite the low scan speed; however, the particle in the pit is immobilized well. These experiments were conducted with the substrates and samples at normal lab humidity.

Size and form information can be obtained by the optical microscope, with the AFM providing the close-up surface structure. Figure 10 shows an optical image of a 1 mm particle and AFM images of 1 mm and 10 μm particles.

The depth of focus is limited by the high magnification of the microscope, and the resolution limit of 4 μm per pixel means that little information can be gleaned about the microscale surface morphology of the large particles. Also, particles which are 10 μm or smaller would barely be visible with the optical microscope. Figure 10(b) shows an AFM image of a 2 × 2 μm area of the 1-mm-diameter particle. Fine detail of the surface texture can be observed, with a roughness measured at 200 nm. These features taken with the contextual data from the optical microscope image in Fig. 10(a) suggests that this particle is not of an aquatic origin; however, further deductions would require additional images at different length scales. In Fig. 10(c), the 10 × 10 μm AFM image shows a 8 μm-

diameter particle perched on one of the pits on the etched substrate. Such a particle would be visible in the OM merely as a couple of pixels in the image but the AFM data allows the determination of the particle size (1.3 μm high, 8 μm wide), shape and roughness surface (850 nm). Furthermore, the observed surface texture, which includes a number of parallel linear features, may be the imprint of an aqueous environment on this particular grain, as suggested by the work of Kempe *et al.* (2004). This clearly demonstrates the importance and utility of the AFM in investigating particles in this size range. The quality of the image shows that appropriate scanning parameters can be found that allow AFM imaging of particles without unwanted movement of the particles by the scanning tip. The combination of the optical image and the two AFM images in Fig. 10 suitably demonstrate the complementary capabilities of these two microscopes in imaging from the millimetre down to the nanometre scale.

3.5. Adhesion due to humidity and electrostatic charging

Preliminary experiments on the effect of adsorbed water on the samples and substrates appear to support the idea that the sample-substrate adhesion is enhanced by the presence of adsorbed water. We compared samples and flat substrates where one set had been dried in an oven at 150 °C whereas the other was not. We found that the substrates that were dried prior to the deposition of a dried sample, retained the fewest number of particles, especially in the larger (>100 μm) size range. In the case of the dried samples and substrates, we would expect that triboelectric charging of the particles would lead to electrostatic effects that enhance the adhesion between particles and substrates. However, the above experiments show, at least qualitatively, that any effect of electrostatics in assisting adhesion is probably weaker than that of surface tension since dry samples appear to hold fewer particles than wet ones. This has important consequences for the experiments on Mars, as the cold, dry atmosphere at the Martian surface would preclude any adhesion due to surface tension effects. Triboelectric charging would certainly be significant on Mars (Gross *et al.*, 2001; Merrison *et al.*, 2004) although estimates of the magnitude of the charging vary widely. Therefore, in the interest of retaining a greater range of particles on the silicon substrates, the patterned topography appears all the more important.

Further experiments are planned in a Mars environmental chamber which will simulate the low humidity environment expected on Mars and tell us more about the contribution of charging to the adhesion between particles and the substrates and also importantly, to the AFM tip itself.

4. Conclusions

We have shown that adequate sample preparation is essential for the study of sand-like material with large aspect ratios
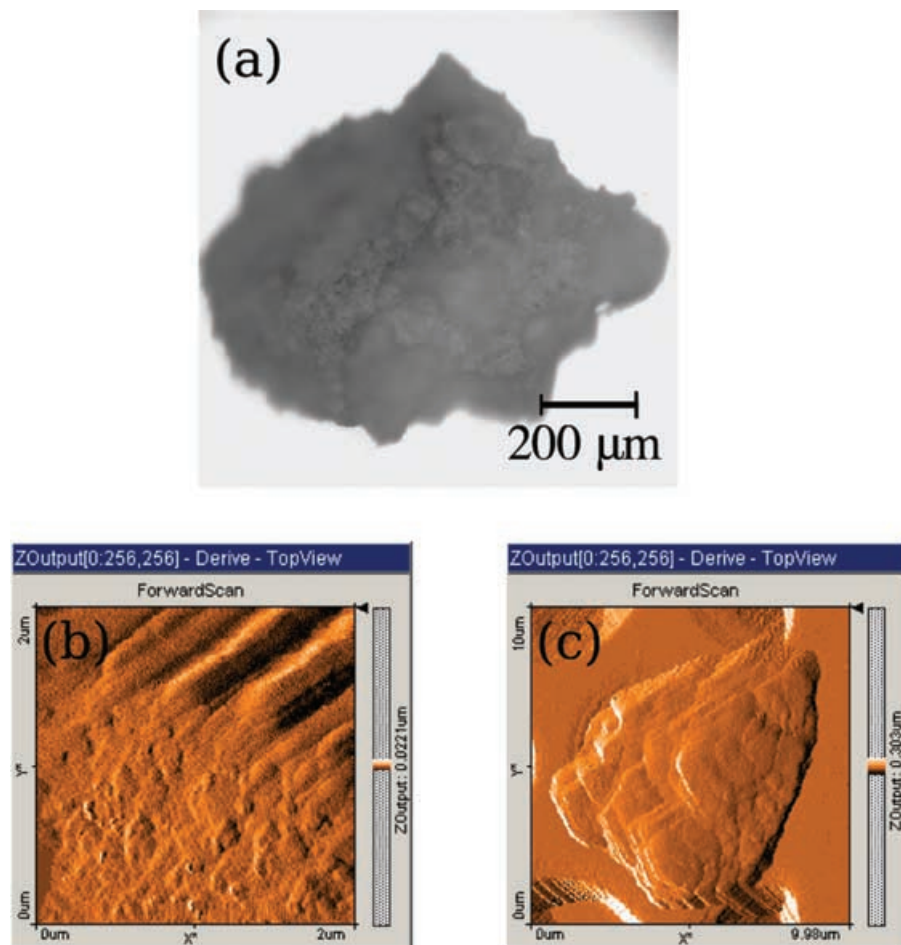
Fig. 10. Caption: (a) Optical microscope image showing what a 1 mm particle would look like at high magnification and at 4 m per pixel resolution. The optical microscope is unable to resolve the finest features on the surface of the large particle. A 10 m particle would be almost invisible at this scale. (b) and (c) are the derivatives of topography images from the AFM demonstrating the fine structure that is resolvable for large and small particles. (b) is a 2 × 2 m scan of a 1 mm particle, whereas (c) shows a 10-m-diameter particle on a pit. These experiments were conducted with the substrates and samples at normal lab humidity.

using the atomic force microscope. This is especially true in the case of future AFM investigations on the Martian surface during the forthcoming NASA Phoenix mission landing in May 2008. One method that has been demonstrated and incorporated into the Phoenix mission is the use of deep reactive ion-etched substrates with pits or pillars to sort and immobilize individual grains. Martian soil simulants in the form of JSC Mars-1, alumina particles and diatomaceous earth have been used to demonstrate the utility of such substrates in preparation for *in situ* experimentation during the Phoenix mission. Our experiments show that micromachined silicon substrates allow substantial control of the sample configuration, enabling safe and successful AFM imaging of micron sized particles. The combination of optical and AFM imaging of micron-sized particles and larger in their entirety or in part will be useful for the gleaning of information on dust and soil particle sizes, shapes and weathering processes, whether on Earth or on Mars.

performance. The magnetic substrates described here were contributed by the Niels Bohr Institute at the University of Copenhagen. MECA's optical microscope was developed by the University of Arizona, with the camera electronics contributed by the Max Planck Institute for Solar System Research. We also thank NASA Jet Propulsion Laboratory for integration and management.

Finally, we would like to thank Peter Smith, the PI of the Phoenix mission for this great opportunity to be involved with Phoenix.

References

Akiyama, T., Gautsch, S., de Rooij, N.F. *et al.* (2001) Atomic force microscope for planetary applications. Sensors Actuators, A **91**(3), 321–325.

Allen, C.C., Morris, R.V., Lindstrom, D.J., Lindstrom, M.M., Lockwood, J.P. (1997) JSC Mars-1: Martian regolith simulant. *Lunar Planet. Inst. Conf. Abstracts* **28**, 27.

Barkay, Z. (2005) Atomic force and scanning electron microscopy of atmospheric particles. *Micros. Res. Tech.* **68**, 107–114.

Bhushan, B., Kasai, T., Nguyen, C.V. & Meyyappan, M. (2004) Multiwalled carbon nanotube AFM probes for surface characterization of micro/nanostructures. *Microsyst. Technol.* **10**(2004), 633–639.

Gautsch, S., Akiyama, T., Imer, R. *et al.* (2002) Measurement of quartz particles by means of an atomic force microscope for planetary exploration. *Surf. Interface Anal.* **33**, 163–167.

Gierasch, P.J. & Goody, R.M. (1968) A study of the thermal and dynamical structure of the Martian lower atmosphere. *Planet. Space Sci.* **16**, 615–646.

Gross, F.B., Grek, S.B., Calle, C.I. & Leeb, R.U. (2001) JSC Mars-1 Martian Regolith simulant particle charging experiments in a low pressure environment. *J Electrostat.* **53**, 257–266.

Horneck, G., Facius, R., Reitz, G., Rettberg, P., Baumstark-Khan, C. & Gerzer, R. (2001) Critical issues in connection with human planetary missions: protection of and from the environment. *Acta. Astronautica* **49**(3–10), 279–288.

Hosaka, S., Morimotob, T., Kurodab, H., Minomotob, Y., Kembob, Y. & Koyabuc, H. (2002) New AFM imaging for observing a high aspect structure. *Appl. Surf. Science* **188**, 467–473.

Kahn, R.A., Martin, T.Z., Zurek, R.W. & Lee, S.W. (1992) The Martian dust cycle, Mars. (ed. by H.H. Kieffer, *et al.*), pp. 1017–1053, Univ. of Ariz. Press, Tucson, AZ.

Kempe, A., Jamitzky, F., Althrmann, W., Baisch, B., Markert, T. & Heckl, W.M. (2004) Discrimination of Aqueous and aeolian paleoenvironments by atomic force microscopy—a database for the characterization of Martian sediments. *Astrobiology* **4**(1), 51–64.

Landis, G., Jenkins, P., Flatico, J., Oberle, L., Krasowski, M. & Stevenson, S. (1996) Development of a Mars dust characterization instrument. *Planet. Space Sci.* **44**(11), 1425–1433.

Merrison, J., Jensen, J., Kinch, K., Mugford, R. & Nornberg, P. (2004) The electrical properties of Mars analogue dust. *Planet Space Sci.* **52**, 279–290.

Pike, W.T., Ilecht, M.H., Smith, P.H. & Staufer, U. (2001) A microscopy station for Mars. Electron Microscopy and Analysis Proceedings pp. 163–166.

Resch, R., Meltzer, S., Vallant, T. *et al.* (2001) Immobilizing Au nanoparticles on SiO2 surfaces using octadecylsiloxane monolayers. *Langmuir* **17**, 5666–5670.

Ridley, R.S., Strate, C., Cumbo, J., Grebs, T. & Gasser, C. (2002) The implementation of AFM for process monitoring and metrology in trench MOSFET device manufacturing. IEEE /SEMI Advanced Semiconductor Manufacturing Conference, pp. 408–414.

Riedler, W., Torkar, K., Ruedenauer, F. *et al.* (1998) The MIDAS experiment for the Rosetta mission. *Adv. Space. Res.* **21**(11), 1547–1556.

Soderblom, L.A., Anderson, R.C., Arvidson, R.E. *et al.* (2004) Soils of Eagle crater and Meridiani planum at the Opportunity Rover landing site. *Science* **36**(**5702**), 723–1726.

Steele, A., Goddard, D., Beech, I.B., Tapper, R.C., Stapleton, D. & Smith, J.R. (1998) Atomic force microscopy imaging of fragments from the Martian meteorite ALH84001. *J Microsc.* **189**(1), 2–6.